J Sci Food Agric **84**:966–976 (online: 2004)
DOI: 10.1002/jsfa.1731

Chemometrics can be applied to mechanical testing data to characterise stem toughness and stiffness in crop plants

EK Kemsley,[1]* RR Swinhoe,[2] AC Smith,[1] MC McCann[2†] and TL Wang[2]

[1]*Institute of Food Research, Norwich Research Park, Norwich NR4 7UA, UK*
[2]*John Innes Centre, Norwich Research Park, Norwich NR4 7UH, UK*

Abstract: Mechanical tests have been used to assess the engineering properties of pea (*Pisum sativum* L) stems. Measurements were made on plants of three different genotypes at four different stages of development and at five defined locations along the stem. The force–displacement curves obtained were used to estimate values of the engineering properties of toughness and flexural modulus, from cutting and flexure mechanical tests respectively. Specimens of all genotypes showed an increase in toughness with age and generally also with stem height. However, there were marked differences in flexural modulus between genotypes. One genotype, known to exhibit a 'stiff straw' characteristic, showed a consistent increase in modulus with age and stem height, and at and beyond fruiting had substantially the greatest flexural modulus. The remaining genotypes showed decreasing flexural modulus with age. Chemometric methods were used to analyse sets of complete force–displacement curves, following suitable pre-processing to allow the application of linear algebra methods. Whereas univariate consideration of the engineering quantities allowed trends to be observed, multivariate analysis of force–distance curves was able to model empirically the genotype differences so that individual specimens could be largely correctly classified. Examination of some of the model coefficients suggested that the ability to discriminate between genotypes is related to structural features of the specimens and that cutting tests in particular are sensitive to the anatomy of the specimen. This is the first time that chemometric methods have been applied to such data and suggests the potential of mechanical tests combined with multivariate analysis to form the basis of a screening system for phenotypic properties of new lines and varieties.

Keywords: mechanical properties; toughness; stiffness; pea stems; chemometrics

INTRODUCTION

'Canopy collapse' of the pea crop occurs at the end of the growing season in the UK and can result in total crop loss in a wet season. In a study of the forces involved, Holland[1] showed that the canopy collapses owing to the weakness of the stems and petioles of individual plants, due to a lack of so-called standing ability. The *afila* character, which converts leaflets to tendrils, was introduced to the modern crop to increase interaction between individual plants and thus reduce the canopy load; that this character increases yields has been shown in field trials using isogenic lines.[2] However, Holland concluded that the best way to make further improvements was to improve the mechanical attributes of the stems and petioles.

Previous studies on plant mechanical properties have included the examination of natural vibrations in triticale peduncle,[3] the determination of flexural strength of barley culm[4] and the determination of pea stem crushing and shearing forces.[5] There have also been studies on varietal differences in chemical composition[6] and the physics of stem strength.[7] However, there have been no thorough studies relating to standing ability in peas. In his model, Holland predicted that increasing the ratio of the stem wall area to the total cross-sectional area (considering the stem to be a pipe) would improve standing ability, as would an increase in the outer diameter of stems. An increase in the number of cells of types that contain substances with higher values of Young's modulus was also predicted to be advantageous. In the past, standing ability has been studied by simple agronomic observations alone, but instrumental tests for predicting standing ability in peas would be useful.

* Correspondence to: EK Kemsley, Institute of Food Research, Norwich Research Park, Norwich NR4 7UA, UK
E-mail: kate.kemsley@bbsrc.ac.uk
†Present address: Department of Biological Sciences, Purdue University, West Lafayette, IN 47907-2054, USA
Contract/grant sponsor: BBSRC
Contract/grant sponsor: DEFRA (MAFF); contract/grant number: AR0104
Contract/grant sponsor: Royal Society
(*Received 27 March 2002; revised version received 26 June 2003; accepted 9 February 2004*)
Published online 20 May 2004

The mechanical properties of plant organs reflect the anatomy of the tissues, the state of turgor of the cells, the cell wall composition and the distribution of reinforcing polymers such as lignin. Thus we expect the mechanical response of the organ to be complex and inherently multivariate, even in straightforward mechanical tests. In the present study, mechanical tests are used to assess the engineering properties of pea stems. The relationship between the genotype and the mechanical phenotype is explored and the outcomes are compared with literature predictions. We also investigate the novel application of multivariate analysis to force–displacement (F–s) curves and show that a multivariate approach can reveal the relationship between genotype and phenotype more effectively than single, derived mechanical properties.

EXPERIMENTAL

Material

Two separate plantings were made of pea (*Pisum sativum* L) plants of three John Innes accessions: JI1183 ('stiff straw'), JI820 and JI64. These lines were drawn from the germplasm collection as representing respectively an agronomic line identified as having a stiff straw, a line expressing a mutation (fasciation) that modifies stem structure, and a line representing the wild scrambling pea. In all cases, measurements were made at four different stages of development: 4 weeks after planting (A), start of flowering (B), start of fruiting (C) and end of fruiting (D); and at five defined locations along the stem: above scale leaf ('asl'), internode 2 ('i2'), internode 15 ('i15'), internode 17 ('i17') and 'top'. These stages represent points at which major changes occur in the canopy and at which changes in stem architecture occur (data to be presented elsewhere).

Mechanical tests

Two types of mechanical test were performed: cutting and flexure. These were carried out using a universal test machine (TA-XT2 texture analyzer, Stable Micro Systems, Godalming, UK) with a 25 kg load cell and a constant crosshead speed of $0.1\,\mathrm{mm\,s^{-1}}$. The cutting tests employed a razor blade (dimensions 39 mm × 13 mm × 0.20 mm) attached to the crosshead. The flexure tests were carried out using a three-point bend geometry. The test jig comprised two parallel bars (0.5 mm radius) on which the pea stem was placed orthogonal to the bars. A third parallel bar (0.5 mm radius), offset in the vertical direction and attached to the machine crosshead, was driven down to deflect the stem at midlength. Two geometries were used for the different stages of development as dictated by the length of the internodal region: 8 mm span for asl and i2, and 27 mm span for i15, i17 and top locations.

Cutting tests have been used previously to gain estimates of toughness of plant tissues.[8–10] The three-point bend flexure test is also well documented.[4,11,12] In both types of test the force exerted on the specimen is recorded at a predetermined sampling rate, giving rise to a vector measurement from each specimen. Each vector element represents the measured force at a particular displacement of the crosshead and can be viewed graphically as a force versus displacement (F–s) curve. The engineering properties of toughness and flexural modulus can be approximated from F–s curves obtained during cutting and flexure tests respectively.

Both the cutting and flexure tests were destructive—once a plant had been analysed at a particular developmental stage, it was destroyed. The schemes for data collection are shown in Tables 1 and 2.

Stem structure and geometry

Following each measurement in the cutting test, a fresh hand-cut stem section was taken, stained with toluidene blue according to O'Brien *et al*,[13] then photographed using a Leica (Milton Keynes, UK) MZ8 stereomicroscope. Stem diameters were measured from these images. For hollow stems a measurement was also made of the diameter of the hollow section. Owing to the destructive nature of the bending test, stem sections could not be obtained and therefore diameter measurements were made using callipers before each test.

Table 1. Scheme for data collection from each genotype (cutting tests). Total number of F–s curves recorded = 570

Stem location	Developmental stage			
	A	B	C	D
top				15 (3 tests on each of 5 plants)
i17			15 (3 tests on each of 5 plants)	15 (3 tests on each of 5 plants)
i15		15 (3 tests on each of 5 plants)	15 (3 tests on each of 5 plants)	15 (3 tests on each of 5 plants)
i2	15 (3 tests on each of 5 plants)	15 (3 tests on each of 5 plants)	15 (3 tests on each of 5 plants)	15 (3 tests on each of 5 plants)
asl	10 (2 tests on each of 5 plants)	10 (2 tests on each of 5 plants)	10 (2 tests on each of 5 plants)	10 (2 tests on each of 5 plants)

Table 2. Scheme for data collection from each genotype (flexure tests). Total number of $F-s$ curves recorded = 420

Stem location	Developmental stage			
	A	B	C	D
top				10 (1 test on each of 10 plants)
i17			10 (1 test on each of 10 plants)	10 (1 test on each of 10 plants)
i15		10 (1 test on each of 10 plants)	10 (1 test on each of 10 plants)	10 (1 test on each of 10 plants)
i2	10 (1 test on each of 10 plants)	10 (1 test on each of 10 plants)	10 (1 test on each of 10 plants)	10 (1 test on each of 10 plants)
asl	10 (1 test on each of 10 plants)	10 (1 test on each of 10 plants)	10 (1 test on each of 10 plants)	10 (1 test on each of 10 plants)

Chemometric analysis

All data analysis was carried out using the Matlab matrix programming language (The Mathworks Inc, Natick, MA, USA). Pre-processing of $F-s$ curves from the cutting tests and of the greyscale image data was carried out using Matlab's inbuilt interpolation routines. In general, the $F-s$ curves collected in the study each contained several hundred discrete data values. Such data, where the dimensions of each vector measurement are large, are described as high-dimensional; a family of multivariate techniques, known as chemometrics, is especially suitable for handling data of this kind. For the analysis of complete $F-s$ curves a combination of chemometric methods was employed to model the three-genotype group structure: discriminant partial least squares (PLS) followed by linear discriminant analysis (LDA) using the Mahalanobis distance metric.[14] Discriminant PLS is a form of PLS regression in which the regressands are binary 'dummy' variates encoded with the proposed group structure. Matlab algorithms were written in-house to carry out PLS/LDA for a range of model dimensionalities (numbers of PLS scores), using internal cross-validation throughout. PLS/LDA was also applied to the greyscale intensity data obtained from the optical microscopy images, again with the aim of discriminating between genotypes.

RESULTS AND DISCUSSION

Stem diameter measurements

The outer stem diameter measurements are summarised by box and whisker plots for each of the three genotypes at each location and developmental stage (Fig 1). Some trends can be observed. The mean stem diameter tends to increase with the height of the measurement location in all genotypes and at any developmental stage. The pea stem thus forms an inverted pyramid structure. JI64 shows consistently the lowest mean stem diameter, comparing genotypes at the same location and developmental stage. JI820 shows consistently the greatest mean stem diameter. This is perhaps surprising, since it is JI1183 that is listed in the John Innes pea germplasm collection as having a 'stiff straw' character, and this finding therefore runs counter to Holland's[1] predictions, which suggest that stem diameter should be a primary predictor of good standing ability. At many locations and developmental stages the systematic differences between genotypes are sufficient for the stem diameter alone to be a good indicator of the genotype of individual specimens.

In the assessment of stem morphology, solid stems were found at the lowest two locations (asl and i2) and hollow stems at location i15 and above in all three genotypes.

Cutting of stems

Subsets of the $F-s$ curves obtained by cutting are shown in Fig 2. Owing to gross differences in stem thickness, the $F-s$ curves extend over a range of different maximum displacements. There is also considerable variability in the shape of the curves, although there are some common features. In many of the curves the force shows a local maximum (such as that marked with an asterisk) when it first penetrates the surface of the stem—this represents the initial resistance to cutting. Owing to friction between the blade and the specimen, the force thereafter generally increases with displacement, reaching one or more large, fairly broad maxima, before decreasing again as the stem nears failure.

The complete set of 570 $F-s$ curves was examined visually and there were found to be two main, typical peak patterns. Some of the curves show a single broad maximum (such as the majority of those shown in Figs 2(a)–2(c)), occurring at a displacement very approximately half the stem thickness; this curve shape is typically found at the two lowest stem locations. Other curves exhibit two maxima, such as the majority of those shown in Fig 2(d). We interpret these different curve shapes as arising from solid and hollow stems respectively. However, curves were also obtained that did not match either of these typical patterns. This may be due to factors such as variable compression of the stem and differences in the ratio of the outer to inner diameters, all of which are likely to affect the shape of the $F-s$ curve.

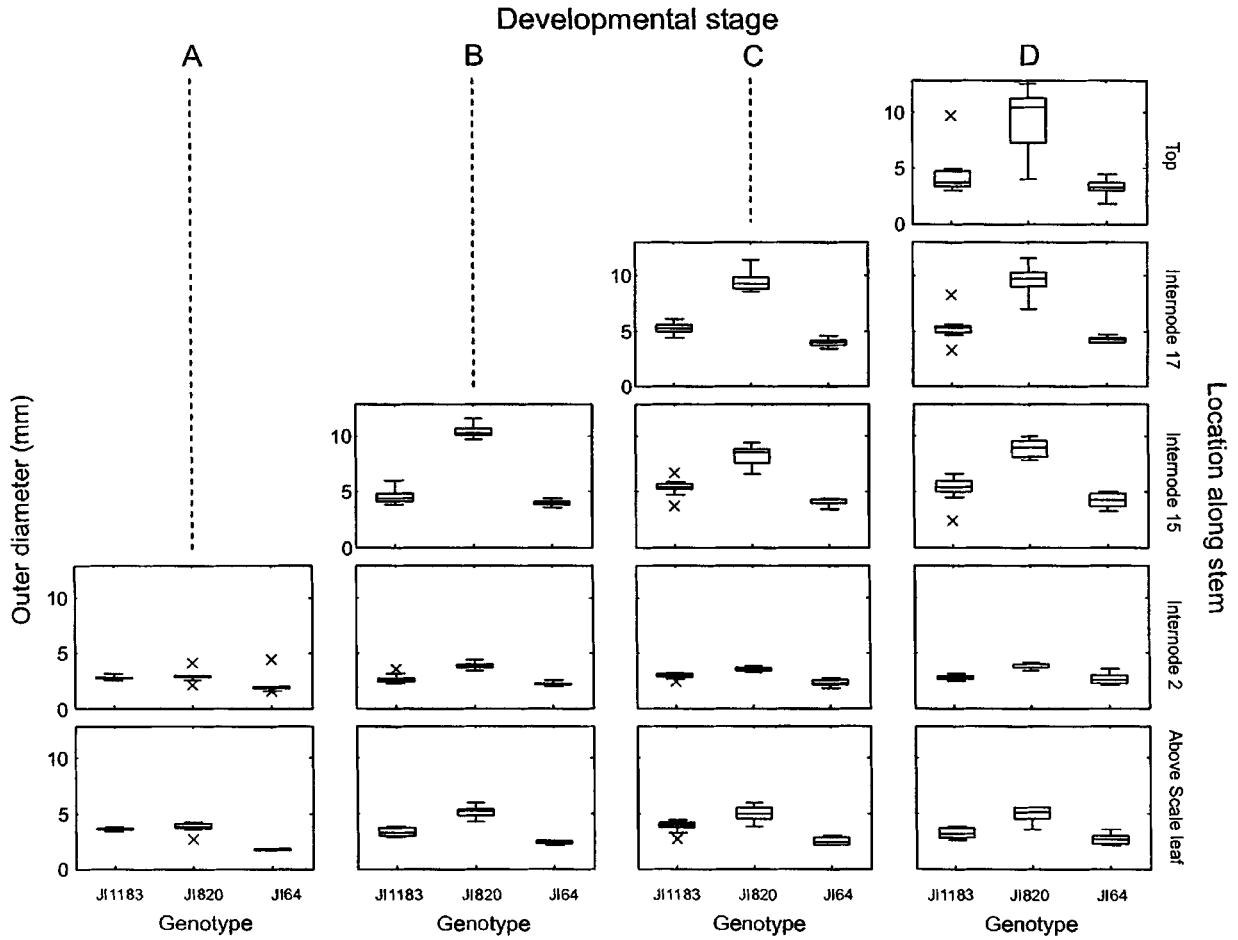

Figure 1. Box and whisker plots for the outer stem diameter measurements. The box has lines at the lower quartile, median and upper quartile values. The whiskers extend to the most extreme data value within two times the interquartile range of the box. Outliers lying beyond the ends of the whiskers are marked with a cross. Refer to Tables 1 and 2 for the numbers of measurements made for each genotype, stem location and developmental stage.

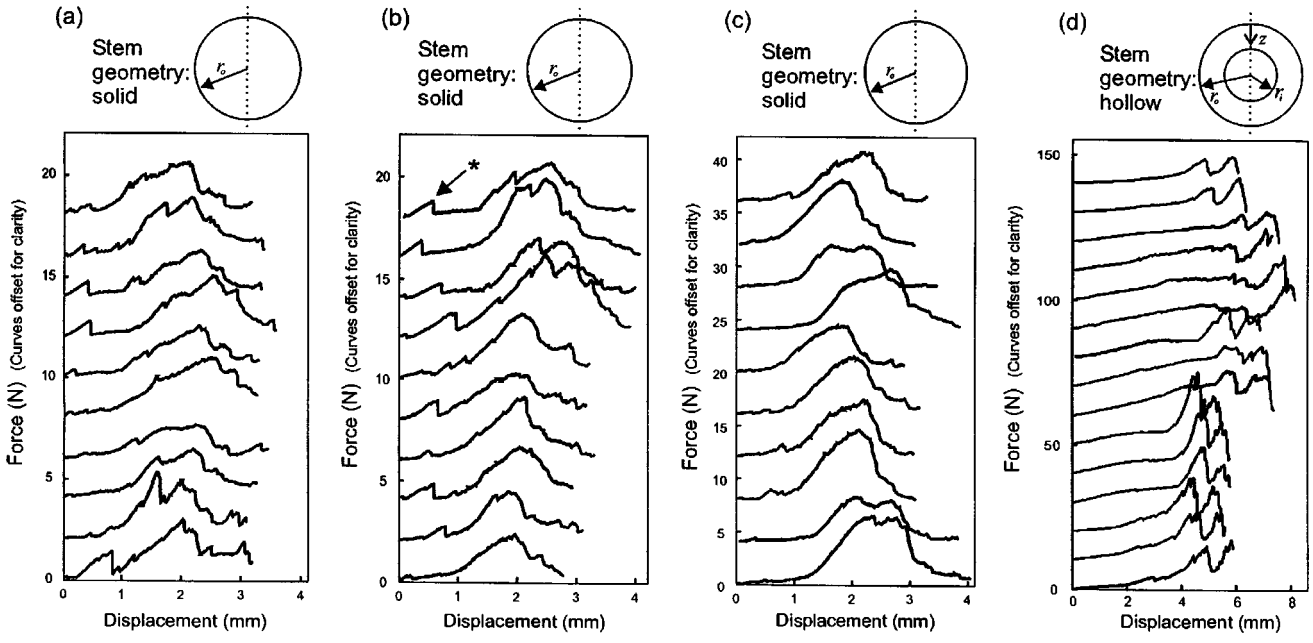

Figure 2. Some typical force–displacement (F–s) curves obtained by cutting, and schematic of the corresponding stem type: (a) JI1183, developmental stage A, location asl; (b) JI820, developmental stage A, location asl; (c) JI1183, developmental stage D, location asl; (d) JI820, developmental stage D, location i17.

A measure of the stem toughness was calculated from each F–s curve. Toughness is defined as the energy required to create unit new cut area. While this energy is often taken as the area under the F–s curve corresponding to a known cut area, this is an overestimate, since not all of this energy goes into creating a new surface.[12] For rectangular section specimens the energy needed to create unit new cut area reduces to the equilibrium force divided by the specimen width.[15] The geometry of pea stems, however, is more complex. For a solid, circular section beam the area cut is determined by the chord length; for a hollow pipe there is an additional dependence on the diameter of the internal hollow core (see Fig 2(d)). It can be shown that the cut area A as a function of the distance z is given by

$$A(z) = A_o(z) - \Phi(r_i - r_o + z)\Phi(r_i + r_o - z)A_i(z) - \Phi(z - r_i - r_o)A_i(r_i + r_o)$$

in which Φ represents a Heaviside step function ($\Phi(t) = 0$ for $t \leq 0$, $\Phi(t) = 1$ for $t > 0$), with

$$A_o(z) = r_o^2.\cos^{-1}\left(1 - \frac{z}{r_o}\right) - (r_o - z)(2r_o z - z^2)^{0.5}$$

and

$$A_i(z) = r_i^2.\cos^{-1}\left(\frac{r_o - z}{r_i}\right) - (r_o - z)(r_i^2 - r_o^2 + 2r_o z - z^2)^{0.5}$$

where r_i and r_o are the inner and outer radii respectively. We have elected to estimate the toughness T as a function of z as follows:

$$T(z) = \frac{\int_0^z F(u).\mathrm{d}u}{A(z)}$$

where the definite integral is obtained from the F–s curve. In the case of a pea stem, however, the compression of hollow stems can, *in extremis*, convert the circular annular section into a solid elliptical section. From comparing the measured diameters with the maximum distance s_{max} travelled by the cutting edge, it was clear that a degree of compression of the stem was occurring during some of the measurements. Therefore, to calculate $A(z)$, the values of r_o and r_i have first been scaled using the maximum travel of the cutting edge; thus

$$r_o = \frac{d_o}{2}.\frac{s_{max}}{d_o}, \qquad r_i = \frac{d_i}{2}.\frac{s_{max}}{d_o}$$

where d_o and d_i are the measured outer and inner diameters respectively ($d_i = 0$ for solid stems). Owing to these various considerations, it is apparent that the 'true' toughness of real specimens can only be approximated by quantities derived from the F–s curve.

Box and whisker plots of toughness obtained from each genotype, stem location and developmental stage are shown in Fig 3. For all genotypes the toughness tends to increase with the age of the specimen at all measurement locations. JI820 and JI64 specimens show generally quite similar toughness at all developmental stages, whereas JI1183 becomes comparatively less tough at all stem locations with the age of the specimens. However, within any location or developmental stage the differences are not sufficiently great to allow identification of individuals from their toughness values.

Multivariate analysis of cutting data

Figure 2 illustrates the difficulty of inspecting and analysing a data set of this size and complexity in its raw form. In mathematical terms the force measurements from the jth individual can be regarded as a $1 \times m_j$ row vector $\boldsymbol{\xi}_j$, where m_j is the number of discrete displacements at which data values were collected. Because the stems vary in thickness, m_j is in general different for each vector. This leads immediately to a problem, since, in order for linear algebra techniques to be applied, the $\boldsymbol{\xi}_j$ must be collated into a matrix in a meaningful way: all measurement vectors must contain the same number of elements, so that each column of the matrix represents measurements of the same property on all specimens.

To address this difficulty, we have used cubic interpolation to adjust the values of m_j, so that $m_j = m$ for $j = 1, \ldots, n$, using a suitably chosen value for m. Cubic polynomial functions are fitted piecewise to the data in the measurement vector $\boldsymbol{\xi}_j$. The abscissae are the m_j original discrete displacements. Next, m new abscissae are specified and the functions are evaluated at these values to give the interpolated vector $\mathbf{x}_j$. The interpolated data are then collated into an $n \times m$ matrix $\mathbf{X}$ for application of chemometric techniques. There are two benefits of this procedure: firstly, the data are readily collated into a meaningful matrix allowing the application of linear algebra techniques; secondly, the data are normalised with respect to the stem thickness, so that systematic features within the data set *should now represent architectural similarities* (rather than similarities in stem thickness, which do not appear to be usefully or consistently associated with genotype). We have elected to use $m = 1000$. This ensures that the detail visibly present in the original data is retained, without the interpolated data matrix $\mathbf{X}$ becoming impractically large.

Some examples of the interpolated data are presented in Fig 4. The most obvious visual difference between the curves relates to overall scale, with the data for JI820 showing the greatest force values. In general, the curves appear 'noisy' and it is not clear whether features present in some of the curves are

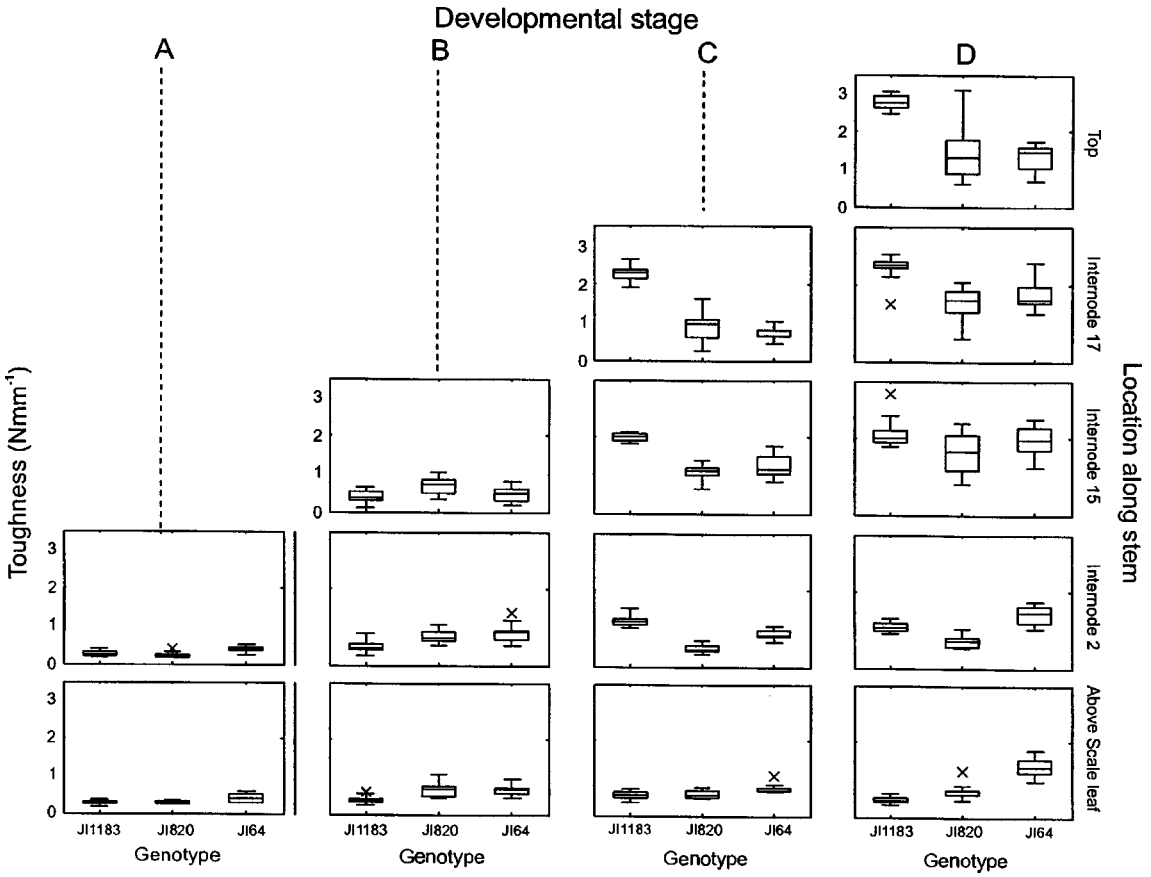

Figure 3. Box and whisker plots for the estimated toughness. See the legend to Fig 1 for definitions of the boxes and whiskers. Refer to Table 1 for the numbers of measurements made for each genotype, stem location and developmental stage.

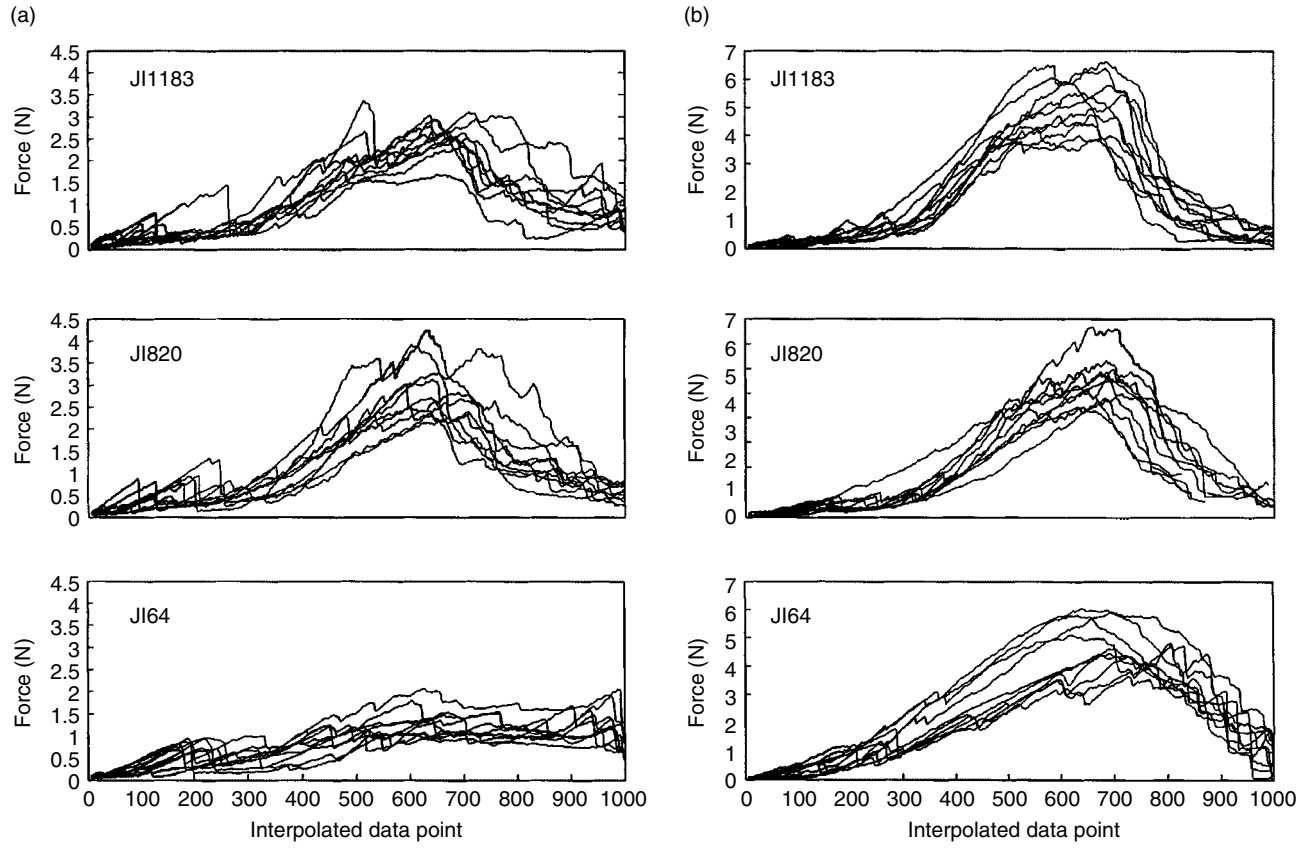

Figure 4. Some examples of interpolated force–displacement (F–s) curves obtained by cutting: (a) developmental stage A, location asl; (b) developmental stage D, location asl.

related to aspects of the sample structure or are simply artefacts. Neither is it possible to discern by eye whether there are systematic differences in curve shape associated with each genotype—further multivariate analysis is required.

PLS/LDA was applied to the data from each combination of location and developmental stage. A primary aim of PLS is to transform data comprising measurements of many properties or 'variates' into a new data set (the PLS 'scores') of much more manageable size. This reduction in complexity is helpful for efficient exploration of large data sets. Moreover, in discriminant PLS the regressands are 'dummy' variates encoded with the proposed group structure. This means that the resulting PLS scores are tailored to the subsequent discriminant analysis step, in which LDA is applied to subsets of the PLS scores to obtain an empirical predictive model of the proposed group structure. PLS/LDA was carried out for a range of model dimensionalities (using from one to 20 PLS scores). In all cases, full, 'leave-one-out' or internal cross-validation (ICV) was used. Extensive studies of ICV in high-dimensional data analysis have shown that it effectively prevents overfitting and gives an unbiased impression of the models' performance.[16] The ICV classification success rates and the numbers of PLS scores used in obtaining these rates are shown in Table 3. Good discrimination between the genotypes is possible in most cases. For some locations and developmental stages the classification ability reaches ~97%. The poorest success rate of 60% is still significantly greater than the mean 'chance' rate (33%) that would be obtained if no group structure were present in the data. We conclude that each genotype corresponds to a mechanical phenotype, which can be largely distinguished using a cutting test combined with multivariate analysis of the $F-s$ data obtained.

It can be seen that the optimum classification success rate is obtained from just two PLS scores for the data from developmental stage D, location i2. For a low-dimensional model like this it can be useful to examine the PLS transformation more closely. Fig 5(a) shows a plot of the first versus second PLS scores obtained by cross-validation. The discrimination between the different genotypes is obvious. Fig 5(b) shows the first two PLS loadings, and Fig 5(c) the data reconstructed from two PLS score–loading pairs. This highlights the systematic differences in the shape of the $F-s$ curves that are enabling the distinction between genotypes. The first PLS dimension largely separates the JI64 specimens from the remaining two genotypes. Loading 1 appears to resemble a mean $F-s$ curve; this is consistent with the finding from the raw $F-s$ curves that generally higher force values are recorded from JI64 specimens.

Table 3. Percentage ICV classification success rates for multivariate analysis of cutting $F-s$ curves. Bracketed figures indicate model dimensionality

Stem location	Developmental stage			
	A	B	C	D
top				82% [7]
i17			75% [11]	87% [7]
i15		67% [4]	93% [7]	91% [8]
i2	69% [4]	93% [8]	82% [3]	96% [2]
asl	87% [4]	97% [6]	60% [6]	90% [2]

The second PLS dimension distinguishes JI1183 from JI820. Loading 2 is more complex in appearance, and we believe it reflects differences in stem anatomy. Evidence for this can be found from analysis of the images obtained by optical microscopy. A rectangular area was defined in each of the images obtained from the 15 different specimens from location i2 and developmental stage D. The areas were stretched within the image analysis software to a constant number of pixels in width (Fig 6(a); this process is the analogue of interpolating to normalise for varying stem diameter). The mean pixel intensities were calculated to give vectors of values to represent the one-dimensional variation in greyscale intensity in the z direction (across the diameter of each stem). Internally cross-validated discriminant PLS was applied to the data from JI1183 and JI820 to focus on the difference between these two groups of specimens. The scores show a clear distinction between the two genotypes in the first PLS dimension. The loading associated with this dimension is shown in Fig 6(b); superposed on this plot is the loading obtained from the analysis of the cutting data. The similarity in form (number, width and relative locations of bands) of these two loadings is clear. We believe this is evidence that the anatomical differences, clearly visible in optical images of the stem, are also responsible for the ability of the cutting tests to distinguish between genotypes.

Bending of stems

A representative selection of the $F-s$ curves obtained by flexure is shown in Fig 7. The curves are typically fairly linear for the low values of displacement shown here ($s < 0.8$ mm, the 'elastic' region), but with increasing displacement show increased curvature (the 'inelastic' region). The slope $\mathrm{d}F/\mathrm{d}s$ in the elastic region was estimated for each curve and used to calculate the flexural modulus according to the expression

$$E = \frac{4L^3}{3\pi(d_o^4 - d_i^4)} \frac{\mathrm{d}F}{\mathrm{d}s}$$

where L is the span[17] and d_o and d_i are the outer and inner stem diameters respectively (for solid stems, $d_i = 0$).

Box and whisker plots for the flexural modulus obtained from each genotype and stem location are shown in Fig 8. The most noticeable trend is that for

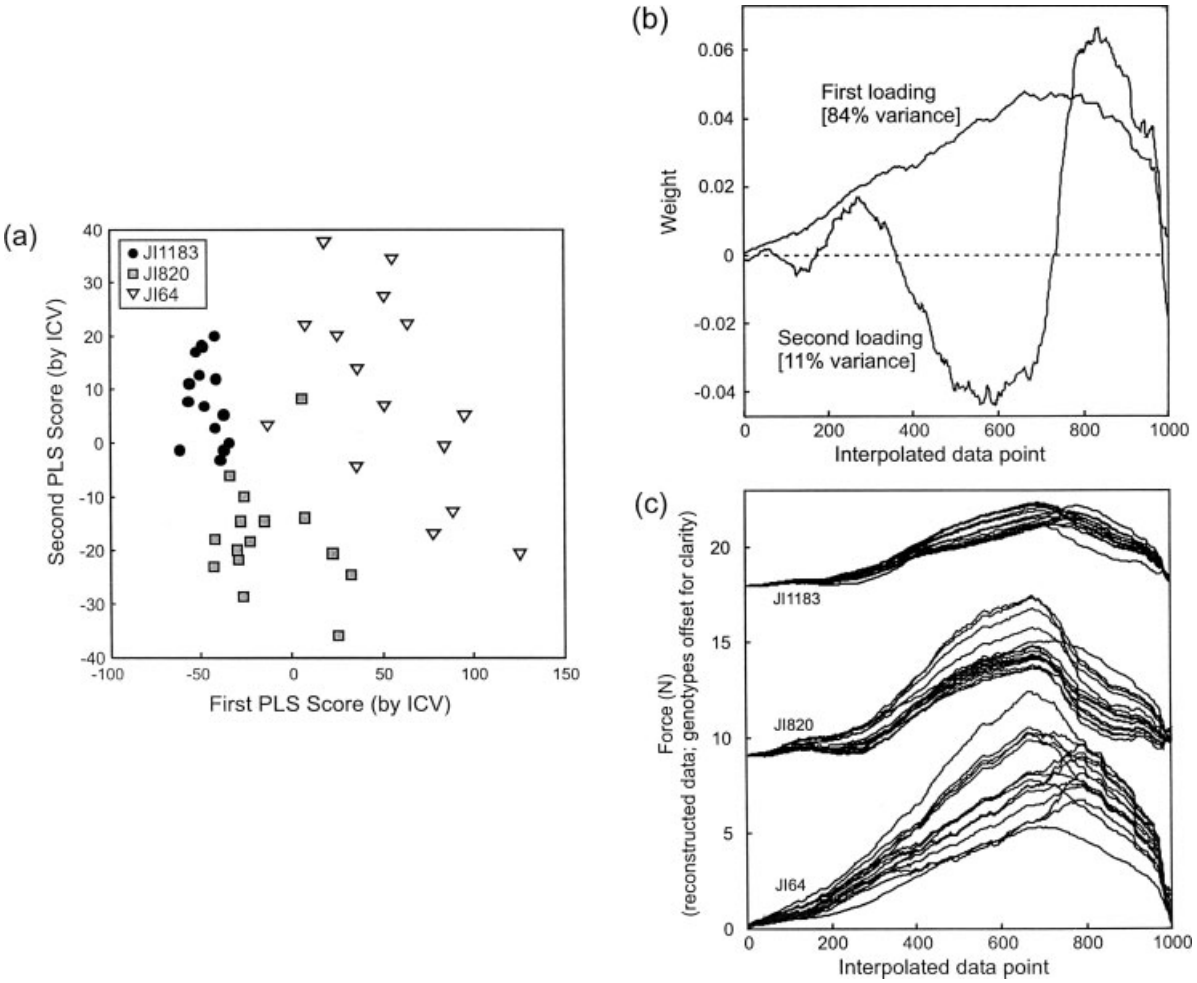

Figure 5. (a) First versus second PLS scores for the interpolated force–displacement (*F*–*s*) curves obtained from developmental stage D, location i2 (internally cross-validated); (b) first two PLS loadings of the data from developmental stage D, location i2; (c) data reconstructed from two PLS score–loading pairs.

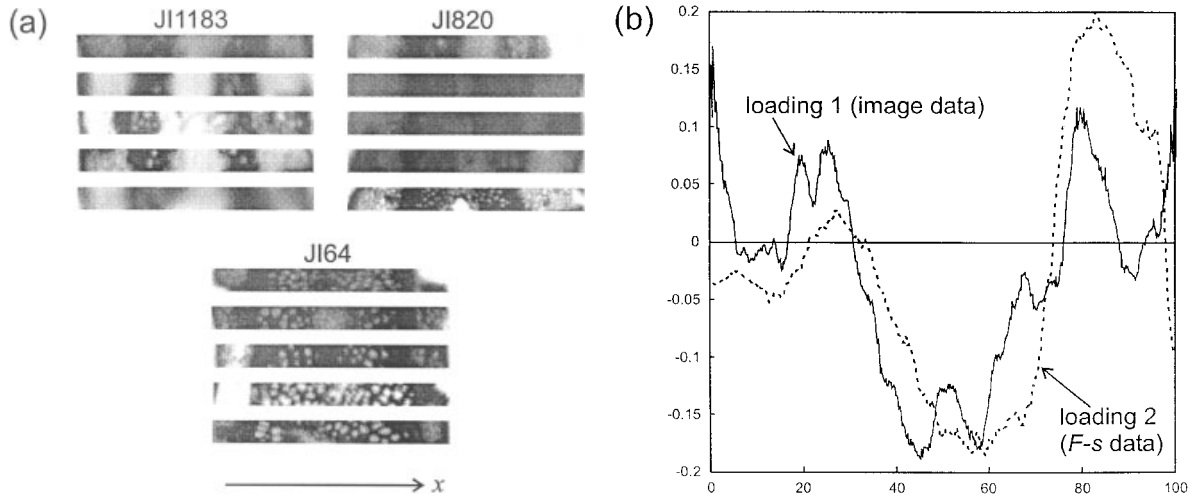

Figure 6. (a) Rectangular area extracted from the images of the stem cross-sections, stretched to constant width; (b) the first PLS loading obtained from the greyscale data, compared with the second PLS loading obtained from the force–displacement (*F*–*s*) data (developmental stage D, location i2).

JI1183 specimens the mean flexural modulus *increases consistently* with developmental stage and location, whereas for the other two genotypes there is generally a decrease with developmental stage and, within each stage, a less consistent increase with location. High flexural modulus is interpreted as high stiffness, so the differences in the flexural modulus between genotypes at developmental stage D are consistent with the known phenotypic characters at harvesting (recall that JI1183 is the 'stiff straw' genotype). It is interesting to

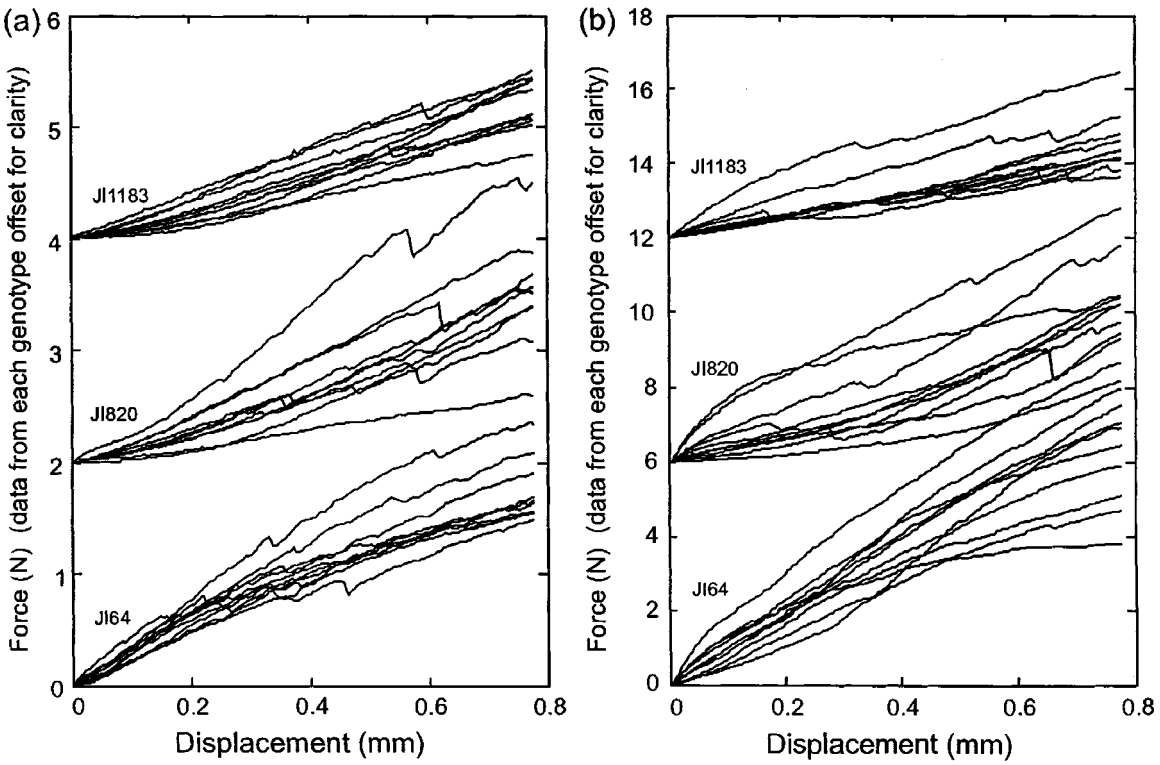

Figure 7. Some typical force–displacement (*F*–*s*) curves obtained by flexure: (a) developmental stage A, location asl; (b) developmental stage D, location asl.

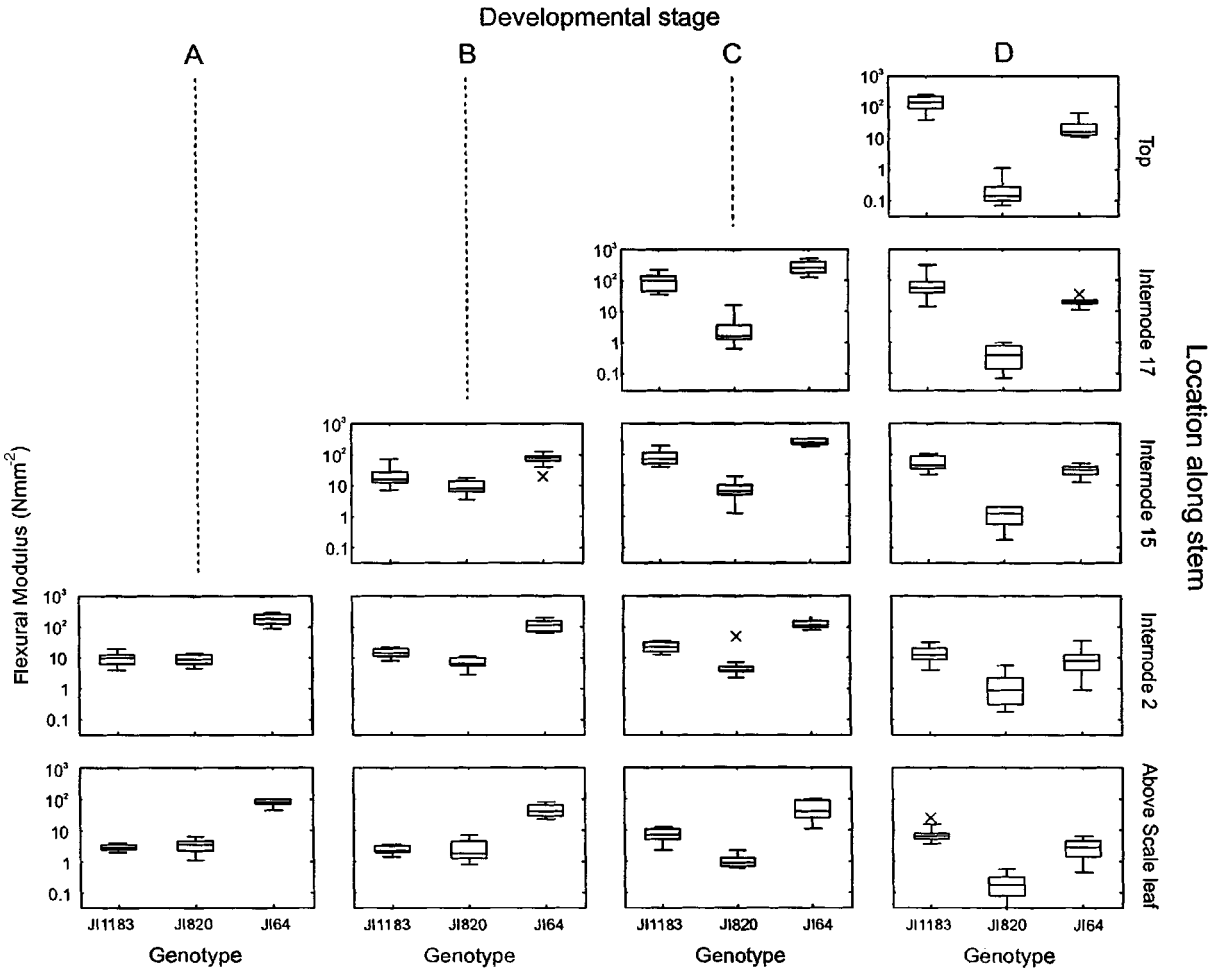

Figure 8. Box and whisker plots of the flexural modulus for each genotype, stem location and developmental stage. See the legend to Fig 1 for definitions of the boxes and whiskers. Refer to Table 2 for the numbers of measurements made for each genotype, stem location and developmental stage.

note that at the earliest developmental stages, however, JI1183 genotype has a very similar flexural modulus to JI820, and both are substantially lower than JI64.

Multivariate analysis of bending data

Multivariate analysis of the $F-s$ curves obtained by flexure was also carried out using PLS/LDA. The region corresponding to $s < 0.8$ mm was used. The classification success rates obtained (Table 4) were overall somewhat more consistent than for the cutting $F-s$ data: the maximum success rate obtained from any combination of location and developmental stage was ~97%, whilst even the poorest model was able to correctly identify 70% of the ICV segments. These results confirm that the genotype is associated with a mechanical phenotype, here identified by differences in the flexural modulus. In addition, multivariate analysis offers more in terms of empirical predictive performance than univariate consideration of the flexural modulus alone. This indicates that the slight variations in $F-s$ curve shape in the $s < 0.8$ mm region carry additional useful information, which is lost in the calculation of a single, derived quantity.

CONCLUSIONS

Both cutting and bending tests are able to highlight differences in the mechanical properties of pea stems. Simple analysis of conventional engineering quantities suggests that specimens of all genotypes increase in toughness with age and generally also with stem height; and JI1183 specimens exhibit generally the lowest toughness. The flexural modulus shows a very different pattern of change for the three genotypes. JI1183 shows a consistent increase with age and stem height, and at fruiting and after fruiting has a substantially greater flexural modulus than JI820 or JI64—it is substantially stiffer. JI820 and JI64 become less stiff with age.

Examination of conventional mechanical properties allows trends to be studied but does not allow individuals of each genotype to be positively identified. Furthermore, crude single properties derived from the $F-s$ curves neglect the fact that the specimens are neither homogeneous nor of simple cross-sectional shape. In contrast, multivariate analysis of complete $F-s$ curves was able to model empirically the genotype differences, so that individual specimens can for the most part be classified correctly. We believe this demonstrates the potential of mechanical tests, in combination with multivariate predictive models, to form the basis of a screening system for evaluating the phenotypic properties of new lines and varieties. Furthermore, examination of some of the coefficients obtained from the cutting data models suggests that the ability to discriminate between genotypes is related to structural features of the specimens, as revealed by optical imaging. We conclude that cutting tests and the $F-s$ curves obtained are sensitive to the anatomy of the specimen.

Table 4. Percentage ICV classification success rates for multivariate analysis of flexure $F-s$ curves. Bracketed figures indicate model dimensionality

Stem location	Developmental stage			
	A	B	C	D
top				87% [2]
i17			70% [8]	80% [5]
i15		70% [3]	90% [4]	77% [3]
i2	97% [4]	90% [2]	90% [2]	77% [3]
asl	70% [2]	77% [6]	70% [2]	80% [3]

ACKNOWLEDGEMENTS

This work was partially funded by the BBSRC's CSG grant (ACS and EKK). TLW, RRS and MCM are grateful for support from DEFRA (MAFF) under Arable Crops research project AR0104. MCM is also grateful to the Royal Society for a University Research Fellowship.

REFERENCES

1 Holland MR, Canopy collapse of dried-pea crops. *PhD Thesis*, University of Edinburgh, pp 61–68 (1998).
2 Stelling D, Performance of morphologically divergent plant types in dried peas (*Pisum sativum*). *J Agric Sci* **123**:357–361 (1994).
3 Zebrowski J, The use of free-vibrations to measure peduncle stiffness in triticale. *J Exp Bot* **42**:1207–1212 (1991).
4 Kokubo A, Kuraishi S and Sakurai N, Culm strength of barley—correlation among maximum bending stress, cell-wall dimensions, and cellulose content. *Plant Physiol* **91**:876–882 (1989).
5 McPhee KE and Muehlbauer FJ, Variation for biomass and residue production by dry pea. *Field Crops Res* **62**:203–212 (1999).
6 Travis AJ, Murison SD, Hirst DJ, Walker KC and Chesson A, Comparison of the anatomy and degradability of straw varieties of wheat and barley that differ in susceptibility to lodging. *J Agric Sci* **127**:1–10 (1996).
7 Oda K, Suzuki M and Udagawa T, Varietal analysis of physical characters in wheat and barley plants relating to lodging and lodging index. *Bull Natl Inst Agric Sci (Nogyo Gijutsu Kenkyujo): Tokyo* **D15**:55–91 (1966).
8 Hiller S and Jeronimidis G, Fracture in potato tuber parenchyma. *J Mater Sci* **31**:2779–2796 (1996).
9 Waldron KW, Smith AC, Parr AJ, Ng A and Parker ML, New approaches to understanding and controlling cell separation in relation to fruit and vegetable texture. *Trends Food Sci Technol* **8**:213–221 (1997).
10 Georget DMR, Smith AC and Waldron KW, Effect of ripening on the mechanical properties of the Portuguese and Spanish varieties of olive (*Olea europaea* L.). *J Sci Food Agric* **81**:448–454 (2001).
11 Brown RP, *Handbook of Plastics Test Methods*. George Godwin, London (1981).

12 Vincent JFV, Fracture properties of plants. *Adv Bot Res Adv Plant Pathol* **17**:235–287 (1990).
13 O'Brien TP, Feder N and McCully ME, Polychromatic staining of plant cell walls by toluidene blue O. *Protoplasma* **59**:367–373 (1964).
14 Kemsley EK, *Discriminant Analysis and Class Modelling of Spectroscopic Data*. Wiley, Chichester (1998).
15 McGarry A, Cellular basis of tissue toughness in carrot (*Daucus carota* L) storage roots. *Ann Bot* **75**:157–163 (1995).
16 Defernez M and Kemsley EK, The use and misuse of chemometrics for treating classification problems. *Trends Anal Chem* **16**:216–221 (1997).
17 Roark RJ and Young WC, *Formulas for Stress and Strain*. McGraw-Hill, New York (1975).